

# Channel Estimation of Correlated Channels in RIS-Assisted Wireless Communication Systems

Ural MUTLU<sup>1</sup>, Yasin KABALCI<sup>2</sup>

<sup>1</sup> Bor Vocational School, Niğde Ömer Halisdemir University, Niğde, TURKIYE

<sup>2</sup> Electrical and Electronics Engineering Department, Niğde Ömer Halisdemir University, Niğde, TURKIYE

Corresponding author: Yasin Kabalci (e-mail: yasinkabalci@ohu.edu.tr).

Submitted on 03.07.2024, Revised on 10.07.2024, Accepted on 10.07.2024, Published online on 22.07.2024

**ABSTRACT** In Reconfigurable Intelligent Surfaces (RIS) aided communication systems, knowledge of the channel state information is critical in optimizing the reflection coefficients of the RIS. However, the existing methods proposed for the non-parametric channel models involve a large training overhead. To reduce the channel estimation overhead, the spatial correlation inherent in the communication systems due to small inter-element distances in the antennas and the RIS as well as the directionality of the antennas can be exploited to group a set of adjacent RIS elements to share a common training reflection coefficient, thus effectively reducing the number of training time slots needed for the channel estimation by a factor of group size. The study defines a correlated channel model for Uniform Linear Array (ULA) and Uniform Planar Array (UPA) antenna arrays and implements a channel estimation algorithm based on the Discrete Fourier Transform (DFT) reflection training pattern at the RIS. The effects of the correlation coefficients and the RIS size on the channel estimation performance are observed. The results show that even at low correlation, the grouping scheme is effective at reducing the training time.

**KEYWORDS** RIS, channel estimation, correlated channel model, element grouping.

## 1. INTRODUCTION

In the last couple of decades, we have seen exponential growth in the research and innovations in wireless communications, which is driven by the increase in demand for higher data rates, lower delays, and increased spectral efficiency. More recently, massive multiple-input-and-multiple-output (MIMO) and millimeter wave (mmWave) communication have been developed to considerably improve the spectral efficiency of the current Fifth Generation (5G) communication networks, as well as the future Beyond 5G (B5G) communication networks. However, both these technologies drastically increase antenna hardware complexity and cost, while also increasing energy consumption. To mitigate some of the MIMO hardware complexities, Reconfigurable Intelligent Surfaces (RIS) have emerged as a complementary energy-efficient and cost-effective technology that can assist MIMO communications [1], [2], [3], [4].

RIS is a planar array comprising multiple passive reflecting elements that can adjust the phase and the magnitude of the incident signal with the aim of constructively combining or beamforming the reflected signal in order to improve communication efficiency. The reflection at the RIS is a passive reflection making the RIS a passive device that does not actively use power to generate a transmitted signal. To efficiently beamform

the reflected signals towards the receiver, the reflection coefficients of the RIS elements have to be optimized, however, the optimization of the reflection coefficients requires the Channel State Information (CSI) of the incident and reflected channels to be known by the communication system. Due to the passive nature of the RIS, it does not have an active transceiver that can detect and process training sequences. Therefore, channel estimation for RIS-assisted communication systems becomes a more complex task that is carried out at the base station (BS). Considering that RIS assists the communication between a BS and a User Equipment (UE), a BS can only receive the training signal coming from the RIS, hence it is more practical to determine the UE-RIS-BS channel termed as a cascaded channel rather than determining BS-RIS and RIS-UE channels separately [5], [6].

The proposed channel estimation algorithms for RIS-assisted communication systems are based on two-channel models, mainly structured and unstructured channel models, which are also referred to as parametric and non-parametric channel models [3], [6]. The channels in the sub-6 GHz band are usually assumed to be unstructured or non-parametric channels, hence, each channel is described by an independent and identically distributed complex gain, which reflects both amplitude and phase change of the channel. The

channel estimation algorithms for the unstructured models are simpler but require a longer channel training period resulting in estimation overhead and impractical algorithm. At higher frequencies, the channel models are based on parametric or geometric properties of the channel, such as Angle of Arrival (AoA), Angle of Departure (AoD), complex channel gain, etc, hence the channel models are said to be structured channel models or parametric channel models. The current research studies unstructured channels with correlation properties, therefore, only channel estimation algorithms that deal with the unstructured channels are considered.

One of the initial channel estimation algorithms for RIS-assisted wireless communications is the three-phase ON/OFF method [7]. The three-phase channel estimation algorithm is a widely employed method, where the first phase is the channel estimation or training phase, the second phase is the reflection pattern optimization phase, and the third phase is the data transmission phase. In the ON/OFF method, only one reflection element is turned on for a given time slot while all the other elements are off. Thus, at each time slot, a cascaded channel(s) going through the reflection element that is on is estimated. This method requires the training period to be as long as the number of reflecting elements. There are two drawbacks associated with the ON/OFF method, only a portion of the power is reflected resulting in reduced effective power, and turning off the elements completely may not be practical or possible. To counter the disadvantages, a RIS training reflection pattern based on the Discrete Fourier Transform (DFT) matrix has been proposed [8], [9]. In this method, the reflection coefficients of the RIS elements are assigned to a column of the DFT matrix for a time slot. For consecutive time slots, consecutive columns of the DFT matrix are taken. Due to the orthogonality of the DFT matrix columns, the channel coefficients are obtained at the BS by simply applying the conjugate of the DFT matrix. The DFT method also requires the training time to be at least as long as the number of reflecting elements.

To reduce the channel estimation overhead, the grouping of adjacent RIS elements method so that they share a common training reflection coefficient has been proposed and shown to be an effective method [10], [11], [12], [13]. Due to the close spacing of adjacent antenna elements or RIS elements and the directionality of the antennas [10], [14], [15], [16], a degree of correlation exists between the channels in MIMO communications and it is this correlation that makes grouping of elements a feasible solution. By grouping adjacent RIS elements, rather than estimating the channel properties of the cascaded channels going through each individual RIS element, a single channel coefficient for the group can be estimated, thus reducing the overhead by a factor of

group size. In other words, the number of time slots required to transmit the training sequence would be reduced from  $N$  to  $K$ , where  $N$  is the number of RIS elements and  $K$  is the number of RIS element groups.

Although, channel correlation is the main factor that makes the grouping method an effective channel estimation algorithm, the effects of correlation coefficient on the channel estimation performance have not been reported in the literature. Therefore, the objective of this study is to observe the effects of the degree of correlation on the channel estimation accuracy in RIS-aided MISO communications. More specifically, the study defines the correlated Rayleigh fading channel model based on the Kronecker correlation model and describes how the DFT method can be applied to groups by sharing a reflection coefficient. The simulations are run for correlation coefficients ranging from 0 to 1, showing that even low correlation is sufficient to achieve an acceptable level of channel estimation. The simulations are also run for various RIS sizes and a number of multipaths.

The next section of the study describes the reference RIS-aided communication model and the correlated channel model. Section 3 gives an outline of the channel estimation protocol implemented in the study. Section 4 is the results and discussion section, while section 5 is the conclusion of the study. The notations used in the study are as follows; matrices are denoted as capital letters  $A$  and vectors are given with lowercase bold letters  $\mathbf{a}$ . Matrix transpose, conjugate, and Hermitian operations are  $(\cdot)^T$ ,  $(\cdot)^*$ , and  $(\cdot)^H$ , respectively.  $\otimes$  is the Kronecker product and  $\|\cdot\|_F$  is the Frobenius norm.

## 2. SYSTEM MODEL

The reference model for the RIS-assisted MISO communication system adopted by the study is shown in Fig. 1. The communication system being considered is a MISO communications architecture consisting of a single BS with  $M$  antennas, a single RIS with  $N$  reflecting elements, and a single user with a single antenna.

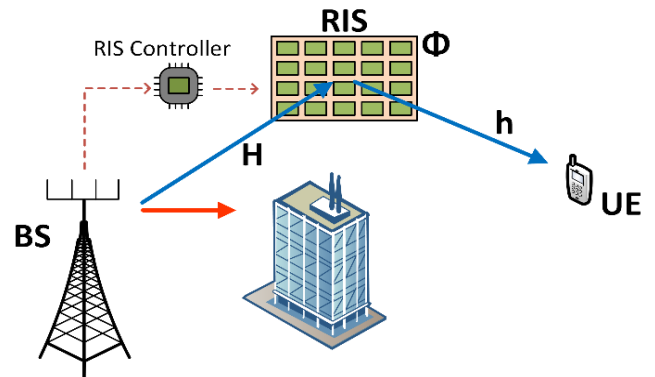


Figure 1. The reference model for RIS-assisted MISO wireless communication system

The RIS is assumed to be passive, *i.e.* it does not have the ability to neither receive nor process signals. Therefore, the channel estimation is carried out at the BS and the channel estimation is a pilot based algorithm, where the UE transmits a training sequence in the uplink and the BS estimates the channel coefficients.

The BS antenna elements are arranged as a horizontal Uniform Linear Array (ULA) and the RIS elements are arranged as a two-dimensional Uniform Planar Array (UPA). The BS and the UE are assumed to contain fully digital transceivers as opposed to analog or hybrid transceivers, in other words, the BS can perform channel estimation for  $M$  antennas in parallel. For simplicity, the BS-RIS direct channel between is assumed to be blocked and the transmitted training signal from the UE to the BS goes through the RIS, *i.e.* only the cascaded channels are available. The BS-RIS channel is shown as  $H \in C^{M \times N}$ , while the cascaded channels are given as  $\mathbf{h} \in C^{N \times 1}$ . The reflection pattern of the RIS is given as  $\Phi = \text{diag}(e^{j\theta_1}, e^{j\theta_2}, \dots, e^{j\theta_N}) \in C^{N \times N}$ , where  $\theta_n \in [0, 2\pi)$  is the  $n^{\text{th}}$  element's reflection phase.

### 2.1. Channel Model

As mentioned in the introduction section, most studies assume the channels in the sub-6 GHz band to be uncorrelated, in practice, the channels tend to have a space-selective fading profile making the channels have a degree of spatial correlation. For the channels to be completely uncorrelated, two conditions must be satisfied; channels are uncorrelated if the channel gains and directions are independent random variables, and the channel directions are uniformly distributed over a unit sphere [14], [15], [17]. However, with the increased number of antenna/RIS elements, the distance between the elements decreases and the antenna elements do not have a uniform radiation pattern. Moreover, the structure of the propagation environment enables some directions to carry stronger signals from the transmitter to the receiver than other directions. Therefore, in instances where the uncorrelated channel conditions are not satisfied, the channels are defined as spatially correlated. Spatial correlation is of particular importance and an unwanted feature in MIMO communications, because, despite improving channel estimation performance, it reduces the channel diversity leading to reduced spectral efficiency.

The channel model adopted in the study is based on the correlated Rayleigh fading channel model [14], [15], [17]. The analytical channel matrix is generated using the Kronecker model, which is a simple spatial correlation model for non-parametric correlated channels in MIMO communications and is based on the assumption that the correlations of the transmit antennas and receive antennas are independent from each other and the correlations for each side are

calculated separately [15], [17], [18]. According to the Kronecker model, the channel matrix is as follows:

$$\mathbf{H} = R_r^{1/2} H_w R_t^{1/2} \quad (1)$$

where,  $H_w \in C^{N_r \times N_t}$  is the uncorrelated MIMO channel, whose elements are modeled as Rayleigh fading and are independent and identically distributed (i.i.d) or  $h_i \sim CN(0,1)$ , where  $h_i$  is a channel in either  $\mathbf{H}$  or  $\mathbf{h}$  and is a Gaussian complex value with zero-mean and unitary variance.  $N_r$  and  $N_t$  represent the number of antennas or in the case of RIS, the number of reflecting elements at the receiver and transmitter side, respectively.  $R_r \in C^{N_r \times N_r}$  and  $R_t \in C^{N_t \times N_t}$  are the spatial correlation matrixes at the transmitter and the receiver, respectively. The spatial correlation matrixes are assumed to be known at the BS [14], [16]. The spatial channel correlation matrixes are characterized in terms of normalized correlation index  $\rho$  [17], [19], [20]. Assuming a ULA antenna array, the correlation matrix and the  $(i, j)$  element in the matrix can be calculated as:

$$r_{i,j} = \rho^{(i-j)^2} \quad (2)$$

$$R = \begin{bmatrix} 1 & \rho & \rho^4 & \dots & \rho^{(n-1)^2} \\ \rho & 1 & \rho & \dots & \vdots \\ \rho^4 & \rho & 1 & \dots & \rho^4 \\ \vdots & \vdots & \vdots & \ddots & \rho \\ \rho^{(n-1)^2} & \dots & \rho^4 & \rho & 1 \end{bmatrix} \quad (3)$$

where,  $n$  is the size of the square matrix. In the case of UPA, as in the RIS, the spatial correlation matrix is dependent on both the horizontal and vertical correlation. Therefore, assuming  $R_x$  and  $R_y$  are horizontal and vertical correlation matrixes for the UPA and the matrixes are generated with (3), the spatial correlation matrix for the UPA can be obtained as a Kronecker product of the two ULA spatial correlation matrices [17]:

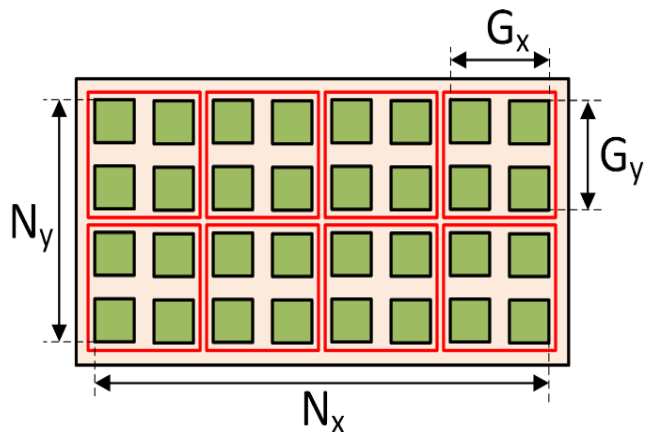


Figure 2. Grouping of RIS elements

$$R_{UPA} = R_x \otimes R_y \quad (4)$$

The methods described up to this point can be used to obtain the BS-RIS channel, which could be shown as  $H = R_{BS}^{1/2} H_w R_{RIS}^{1/2}$ . On the other hand, the RIS-UE channel is a MISO channel and there is only RIS side correlation matrix and the channel model would be:

$$h = R_{RIS}^{1/2} h_w \quad (5)$$

It should be noted that  $R_{RIS}$  for the BS-RIS and RIS-UE channels are not necessarily the same.

### 3. CHANNEL ESTIMATION

The channel estimation algorithm in the study is based on RIS element grouping and using the DFT matrix as a reflection pattern at the RIS. The grouping of RIS elements is displayed in Fig. 2. In the figure,  $N_x$  and  $N_y$  are the number of elements in the horizontal and vertical axes, such that  $N = N_x \times N_y$ .  $G_x$  and  $G_y$  are the number of horizontal and vertical elements in a RIS element grouping and the group size is given as  $G = G_x \times G_y$ . Thus, the number of groups is  $K = N / G$ . For simplicity, we assume  $K$  is an integer.

In the traditional DFT channel estimation method, each RIS element is assigned a reflection coefficient from the DFT matrix, however, in the grouping method, a single reflection coefficient is assigned to the whole group. The channel estimation algorithm is as follows. The UE transmits a training pilot sequence  $x_t$  for time slot  $t$  and the received training signal at the BS is  $y_t \in C^{M \times 1}$ :

$$y_t = H \Phi h x_t + z \quad (6)$$

where,  $z \sim CN(0, \sigma^2)$  is the AWGN noise added at the receiver. To simplify (6), a cascaded channel consisting of BS-RIS and RIS-UE channels is formed as:

$$V = H \cdot \text{diag}(\mathbf{h}) = [v_1, v_2, \dots, v_N] \in C^{M \times N} \quad (7)$$

Each vector in the cascaded channel  $V$  correspond to the cascaded channel going through the  $n^{\text{th}}$  RE. Thus, the received training signal at the BS for time  $t$  is:

$$y_t = V \phi_t x_t + z \quad (8)$$

where,  $\phi = e^{j\theta_1}, e^{j\theta_2}, \dots, e^{j\theta_N} \in C^{N \times 1}$  is the vector of the RIS reflection parameters. In the traditional channel estimation, the reflection pattern is set to  $\Phi = DFT(N)$  and the reflection vectors are taken from consecutive columns from a DFT matrix until all  $N$  columns are used. At the base station,  $N$  received training signals are stacked up to form a received training matrix in the form of  $Y = [y_1, y_2, \dots, y_N] \in C^{M \times N}$ . To obtain the cascaded channel matrix, the orthogonality properties of the DFT matrix are used:

$$\Phi^H Y = \Phi^H V \Phi x + \Phi^H z = V x + \Phi^H z \quad (9)$$

In the grouping method, (9) is modified so that a single training reflection coefficient is applied to a group of RIS elements. In other words, the cascaded channels going through a given RIS grouping would be aggregated at the BS and their coefficients averaged over the group size. Assuming,  $V' \in C^{M \times K}$  is a sub-set of the cascaded channels with the channels corresponding to RIS grouping being aggregated and the grouping reflection pattern is set to  $\hat{\Phi} = DFT(K)$ , by stacking up  $K$  received training signals (9) can be rewritten to obtain  $V'$ :

$$\hat{\Phi}^H Y = \hat{\Phi}^H V \hat{\Phi} x + \hat{\Phi}^H z = V' x + \hat{\Phi}^H z \quad (10)$$

With (10), the training period is reduced from  $N$  to  $K$  time slots. To obtain the full cascaded channel from the sub-set, simply the channels making up the grouping can be assigned the aggregated and averaged value, i.e. the cascaded channels corresponding to the grouping have the same channel coefficient.

### 4. SIMULATIONS AND RESULTS

In this section, the grouping method and the channel estimation algorithms for RIS-assisted communication systems are simulated to observe the effects of spatial channel correlation on the performance of channel estimation. The communication system depicted in Fig. 1 is implemented according to the channel model outlined in Section 2 and the grouping method is applied. The effectiveness of the channel estimation algorithm is evaluated in terms of Normalised Mean Square Error (NMSE). The NMSE is calculated over certain frame transmissions and the MSE is averaged over the total transmitted frames. The equation for NMSE is given as follows, where  $S$  is the number of frames transmitted and  $\hat{V}$  is the estimated cascaded channels.

$$NMSE = \frac{1}{S} \sum_{s=1}^S \frac{\|\hat{V} - V\|_F^2}{\|V\|_F^2} \quad (11)$$

The first simulations observe the effect of the correlation index on the NMSE performance of channel estimation. For the simulation, the number of antennas at the BS is  $M = 4$ , the size of RIS is set to  $N_x \times N_y = 8 \times 8 = 64$ , and the group size is  $G_x \times G_y = 2 \times 2 = 4$ . Thus, channel estimation requires 16 time slots to transmit the training signal. As described in Section 2, there are three spatial correlation matrixes in this study. Initially, all the correlation indexes are assigned equal values.

The results for the NMSE performance of the channel estimation algorithm for various correlation indexes are given in Fig. 3. The correlation index in the figure is

denoted as  $r$  and its value is  $0 \leq r \leq 1$ , where 0 refers to an uncorrelated channel and 1 indicates that all the channels are identical to each other. For  $r=0$  the NMSE value is about 0.75, which is much higher than the acceptable level of  $NMSE = 0.1$  [9]. This result is as expected because the grouping of uncorrelated cascaded channels leads to a loss of channel information, i.e. the channel coefficients are averaged for a given group. For another relatively low correlation index of  $r = 0.05$ , the NMSE value is  $NMSE = 0.12$  and it gets close to the desired value. With another small increase in the correlation index, for  $r = 0.1$  an  $NMSE = 0.085$  is obtained. For the correlation indexes beyond  $r = 0.1$ , there is a clear improvement in the NMSE results. For the threshold value of  $NMSE = 0.1$ , there is 10dB difference between the performances of  $r = 0.1$  and  $r = 0.9$ . At this point, it could be concluded that even low correlation makes the RIS element grouping method a viable channel estimation method for RIS-assisted communication systems.

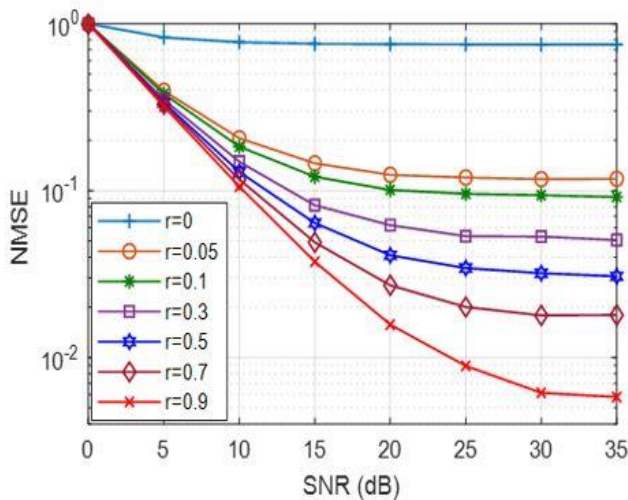


Figure 3. NMSE results for various correlation index values versus SNR

In the Kronecker correlation model, the spatial correlations for the transmitter side and receiver side arrays are independent from each other and the correlation indexes can differ [18]. For example, according to 3GPP, for medium correlation, the correlation index at the BS is 0.3 and at the UE it is 0.9. It could be argued that arrays at the UE are more tightly packed leading to higher correlation index. Therefore, at this point, the study observes the effects of different correlation indexes on the NMSE performance of channel estimation.

The array sizes are as before and the reference point is the case where all three correlation indexes are set to 0.3, and for the other scenarios, the correlation indexes are given in Table 1.

Table 1  
Correlation Scenarios

Scenario	Correlation indexes		
	$r_{BS}$	$r_{RIS1}$	$r_{RIS2}$
Scenario 1	0.3	0.3	0.3
Scenario 2	0	0.3	0.3
Scenario 3	0.9	0.3	0.3
Scenario 4	0.3	0.3	0
Scenario 5	0.3	0.3	0.9
Scenario 6	0.3	0	0.3
Scenario 7	0.3	0.9	0.3

The results for having different correlation indexes for the arrays are displayed in Fig. 4. In the figure, the results for scenarios 1, 2, and 3, the results for scenarios 4 and 6, and the results for scenarios 5 and 7 are almost superimposed. Observing scenarios 1, 2, and 3, the variations in the BS spatial correlation matrix are almost not noticeable in the results. With an array size of 4, the BS array is much smaller than the RIS array with size 64, so the BS spatial correlation matrix does not affect the overall spatial correlation. Scenarios 1, 4, and 5 are carried out to observe the effects of the UE side RIS spatial correlation index, similarly, Scenarios 1, 6, and 7 can be used to compare the effects of the BS side of the RIS spatial correlation index. It is clear from the results that when the RIS correlation index is 0 for both sides, the NMSE performance is the same as NSME for the uncorrelated case in Fig. 3. On the other hand, for a correlation index of 0.9, the results improve. It could be concluded that due to its comparative size to the BS, the spatial correlation matrix of the RIS has a much more significant impact on the results.

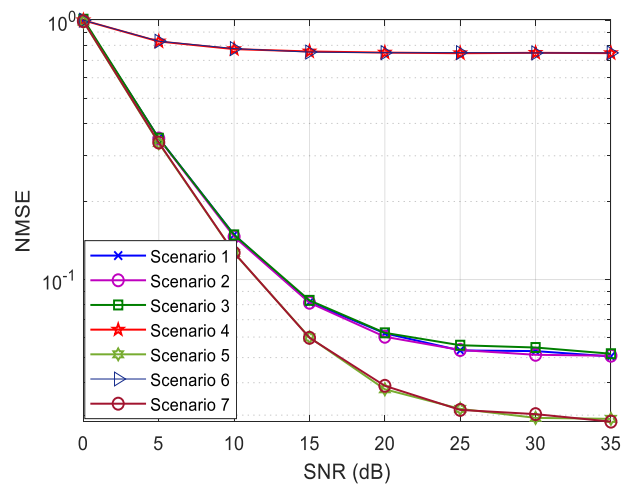


Figure 4. NMSE results for different correlation matrix scenarios versus SNR

The next simulation is carried out to investigate the effects of grouping size on the NMSE of the channel estimation algorithm. The results are depicted in Fig. 5. For the simulations, the RIS array size is still  $N = 64$

elements, and the correlation index is set to  $r = 0.3$  for all the arrays.

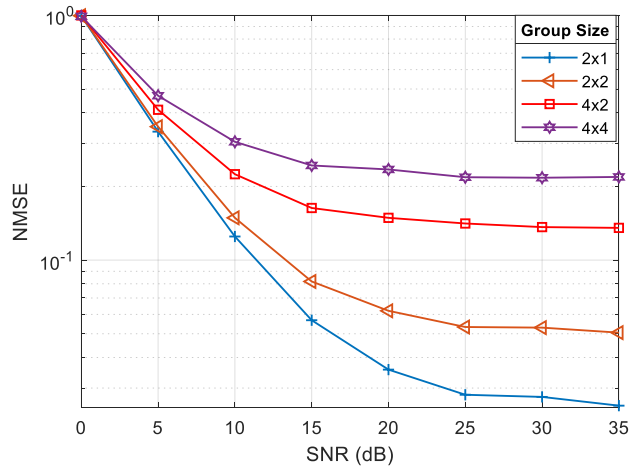


Figure 5. NMSE results for different RIS group sizes

The results show that the NMSE performance is better for smaller group sizes. The results are as expected because with a smaller group size there is less aggregation of channel coefficients.

The last simulation observes the effects of RIS array size on the channel estimation accuracy. The correlation index is set to  $r = 0.3$  for all the arrays and the RIS group size is  $G_x \times G_y = 2 \times 2 = 4$ . The results are displayed in Fig. 6. The results show that the RIS array size has a considerable effect on the NMSE performance of the channel estimation algorithm. (2) and (3) are based on a normalized correlation index and with larger arrays the correlation coefficients of adjacent elements are closer to each other, compared to smaller arrays. In other words, there is a higher degree of correlation between adjacent elements. Therefore, the grouping aggregate of the cascaded channels in larger arrays results in coefficients closer to each individual channel.

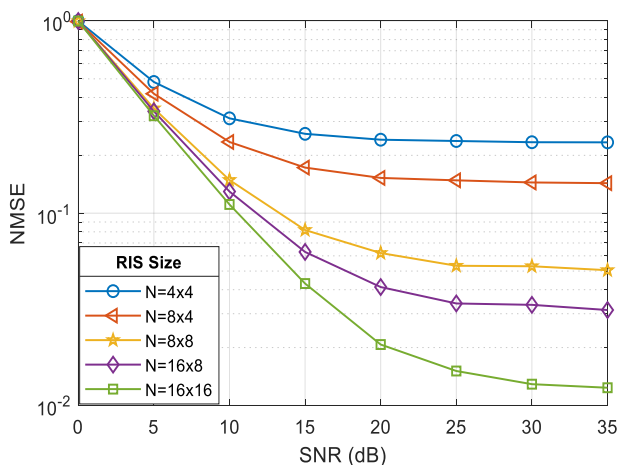


Figure 6. NMSE results for different RIS array sizes

## 5. CONCLUSION

The objective of the study was to observe the effects of spatial correlation on the NMSE performance of the channel estimation algorithm based on RIS reflection element grouping. The results have shown that the grouping algorithm is effective even at low correlation indexes. Since, spatial correlation is a channel characteristic that is known in advance, in cases even with low spatial correlation the algorithm could be applied to reduce the training overhead in RIS-assisted communication systems. Moreover, the grouping algorithm is more efficient with larger arrays, whereas the spatial correlations of much smaller arrays are almost insignificant.

Finally, it should be noted that high spatial correlation is an unwanted feature in MIMO communications as it reduces spatial diversity, but the current study shows that for the purposes of channel estimation in RIS arrays low spatial correlation is an advantage to have.

## REFERENCES

- [1] M. Alsabah *et al.*, '6G Wireless Communications Networks: A Comprehensive Survey', *IEEE Access*, vol. 9, pp. 148191–148243, 2021, doi: 10.1109/ACCESS.2021.3124812.
- [2] B. Zheng, C. You, and R. Zhang, 'Intelligent Reflecting Surface Assisted Multi-User OFDMA: Channel Estimation and Training Design', *IEEE Trans. Wirel. Commun.*, vol. 19, no. 12, pp. 8315–8329, Dec. 2020, doi: 10.1109/TWC.2020.3021434.
- [3] A. L. Swindlehurst, G. Zhou, R. Liu, C. Pan, and M. Li, 'Channel Estimation With Reconfigurable Intelligent Surfaces—A General Framework', *Proc. IEEE*, vol. 110, no. 9, pp. 1312–1338, Sep. 2022, doi: 10.1109/JPROC.2022.3170358.
- [4] U. Mutlu and Y. Kabalci, 'Deep Learning Aided Channel Estimation in Intelligent Reflecting Surfaces', in *2023 5th Global Power, Energy and Communication Conference (GPECOM)*, Nevsehir, Turkey: IEEE, Jun. 2023, pp. 513–518. doi: 10.1109/GPECOM58364.2023.10175750.
- [5] N. K. Kundu and M. R. McKay, 'Channel Estimation for Reconfigurable Intelligent Surface Aided MISO Communications: From LMMSE to Deep Learning Solutions', *IEEE Open J. Commun. Soc.*, vol. 2, pp. 471–487, 2021, doi: 10.1109/OJCOMS.2021.3063171.
- [6] B. Shamasundar, N. Daryanavardan, and A. Nosratinia, 'Channel Training & Estimation for Reconfigurable Intelligent Surfaces: Exposition of Principles, Approaches, and Open Problems', *IEEE Access*, vol. 11, pp. 6717–6734, 2023, doi: 10.1109/ACCESS.2023.3236909.
- [7] D. Mishra and H. Johansson, 'Channel Estimation and Low-complexity Beamforming Design for Passive Intelligent Surface Assisted MISO Wireless Energy Transfer', in *ICASSP 2019 - 2019 IEEE International Conference on Acoustics, Speech and Signal Processing (ICASSP)*, Brighton, United Kingdom: IEEE, May 2019, pp. 4659–4663. doi: 10.1109/ICASSP.2019.8683663.
- [8] T. L. Jensen and E. De Carvalho, 'An Optimal Channel Estimation Scheme for Intelligent Reflecting Surfaces Based on a Minimum Variance Unbiased Estimator', in *ICASSP 2020 - 2020 IEEE International Conference on Acoustics, Speech and Signal Processing (ICASSP)*, Barcelona, Spain: IEEE, May 2020, pp. 5000–5004. doi: 10.1109/ICASSP40776.2020.9053695.
- [9] U. Mutlu and Y. Kabalci, 'Channel Estimation In Intelligent Reflecting Surfaces for 5G and Beyond', in *2022 4th Global Power, Energy and Communication Conference (GPECOM)*, Nevsehir, Turkey: IEEE, Jun. 2022, pp. 586–590. doi: 10.1109/GPECOM55404.2022.9815683.

- [10] B. Zheng and R. Zhang, 'Intelligent Reflecting Surface-Enhanced OFDM: Channel Estimation and Reflection Optimization', *IEEE Wirel. Commun. Lett.*, vol. 9, no. 4, pp. 518–522, Apr. 2020, doi: 10.1109/LWC.2019.2961357.
- [11] N. K. Kundu, Z. Li, J. Rao, S. Shen, M. R. McKay, and R. Murch, 'Optimal Grouping Strategy for Reconfigurable Intelligent Surface Assisted Wireless Communications', *IEEE Wirel. Commun. Lett.*, vol. 11, no. 5, pp. 1082–1086, May 2022, doi: 10.1109/LWC.2022.3156978.
- [12] Z. Li, N. K. Kundu, J. Rao, S. Shen, M. R. McKay, and R. Murch, 'Performance Analysis of RIS-Assisted Communications With Element Grouping and Spatial Correlation', *IEEE Wirel. Commun. Lett.*, vol. 12, no. 4, pp. 630–634, Apr. 2023, doi: 10.1109/LWC.2023.3237232.
- [13] Y. Yang, B. Zheng, S. Zhang, and R. Zhang, 'Intelligent Reflecting Surface Meets OFDM: Protocol Design and Rate Maximization'. arXiv, 2019. doi: 10.48550/ARXIV.1906.09956.
- [14] E. Bjornson, E. G. Larsson, and M. Debbah, 'Massive MIMO for Maximal Spectral Efficiency: How Many Users and Pilots Should Be Allocated?', *IEEE Trans. Wirel. Commun.*, vol. 15, no. 2, pp. 1293–1308, Feb. 2016, doi: 10.1109/TWC.2015.2488634.
- [15] A. Forenza, D. J. Love, and R. W. Heath, 'Simplified Spatial Correlation Models for Clustered MIMO Channels With Different Array Configurations', *IEEE Trans. Veh. Technol.*, vol. 56, no. 4, pp. 1924–1934, Jul. 2007, doi: 10.1109/TVT.2007.897212.
- [16] L. Sanguinetti, E. Bjornson, and J. Hoydis, 'Toward Massive MIMO 2.0: Understanding Spatial Correlation, Interference Suppression, and Pilot Contamination', *IEEE Trans. Commun.*, vol. 68, no. 1, pp. 232–257, Jan. 2020, doi: 10.1109/TCOMM.2019.2945792.
- [17] J. L. Negrão and T. Abrão, 'Efficient detection in uniform linear and planar arrays MIMO systems under spatial correlated channels', *Int. J. Commun. Syst.*, vol. 31, no. 11, p. e3697, Jul. 2018, doi: 10.1002/dac.3697.
- [18] Y. Huang, P. Karadimas, and A. Pour Sohrab, 'Spatial Channel Degrees of Freedom for Optimum Antenna Arrays', *IEEE Trans. Wirel. Commun.*, vol. 22, no. 8, pp. 5129–5144, Aug. 2023, doi: 10.1109/TWC.2022.3231732.
- [19] H. Kim and J. Choi, 'Channel estimation for spatially/temporally correlated massive MIMO systems with one-bit ADCs', *EURASIP J. Wirel. Commun. Netw.*, vol. 2019, no. 1, p. 267, Dec. 2019, doi: 10.1186/s13638-019-1587-x.
- [20] 3GPP TS 36.104 V18.5.0, '3rd Generation Partnership Project; Technical Specification Group Radio Access Network; Evolved Universal Terrestrial Radio Access (E-UTRA); Base Station (BS) radio transmission and reception.' 3GPP, Mar. 2024.